

Effect of chemical substitution on the Néel temperature of multiferroic $\text{Bi}_{1-x}\text{Ca}_x\text{FeO}_3$

Gustau Catalan,¹ Kripasindhu Sardar,² Nathan S. Church,¹ James F. Scott,¹ Richard J. Harrison,¹ and Simon A. T. Redfern¹

¹*Department of Earth Sciences, University of Cambridge, Downing Street, Cambridge CB2 3EQ, United Kingdom*

²*Department of Chemistry, University of Warwick, Coventry CV4 7AL, United Kingdom*

(Received 17 March 2009; revised manuscript received 13 May 2009; published 30 June 2009)

Multiferroic BiFeO_3 ceramics have been doped with Ca and it is found that the magnetic Neel temperature ($T_{\text{Néel}}$) increases as Ca concentration increases, at a rate of 0.66 K per 1% Ca (molar). The smaller ionic size of Ca compared with Bi results in a contraction of the lattice, suggesting that Ca doping can be regarded as a proxy for hydrostatic pressure, with an equivalence of 1% Ca=0.3 GPa. Combining these results, we argue that hydrostatic pressure should increase the magnetic transition temperature of BiFeO_3 at a rate around $\partial T_N / \partial P \sim 2.2$ K/GPa. Our results also suggest that pressure (chemical or hydrostatic) may be used to bring the ferroelectric critical temperature T_c and the magnetic $T_{\text{Néel}}$ closer together, thereby enhancing magnetoelectric coupling, provided that electrical conductivity can be kept sufficiently low.

DOI: [10.1103/PhysRevB.79.212415](https://doi.org/10.1103/PhysRevB.79.212415)

PACS number(s): 75.80.+q

I. INTRODUCTION

Bismuth ferrite BiFeO_3 (BFO) is probably the most intensively studied magnetoelectric multiferroic oxide.¹ Its interest is mainly due to the fact that both the magnetic and ferroelectric orderings take place well above room temperature, with the ferroelectric polarization being among the largest of any ceramic (almost $100 \mu\text{C}/\text{cm}^2$ along the polar $\langle 111 \rangle$ direction^{2,3}). Because of this, it has received an enormous amount of attention, and features of its functional behavior and phase transitions are constantly being uncovered. The temperature-pressure phase diagram of BiFeO_3 , in particular, has proved to be more complex than initially thought, with several phase transitions being reported very recently.^{1,4–7} One difficulty in studying the phase diagram, though, is that key phase transitions such as the ferroelectric-paraelectric or the metal-insulator takes place at either very high temperatures ($T_C=1100$ K and $T_{\text{MI}}=1200$ K, respectively) or pressures (10 GPa and 40–50 GPa, respectively), the latter pressure being only accessible in a handful of laboratories. Because of this, it is useful to extend studies to doped specimens, where the different size of the doping element could have an analogous effect to that of pressure, an effect sometimes called “chemical pressure.”

Studies of chemically substituted BFO abound in the literature. A popular doping element is La substituting for Bi (Refs. 8–12); La and Bi are almost exactly the same size, and this facilitates the substitution while helping stabilize the perovskite phase. There has also been research on the use of tetravalent substitutes for Fe^{+3} so that oxidation is favored as a charge-compensation mechanism, thus minimizing the presence of oxygen vacancies and associated leakage.^{13,14} From the structural point of view, there is also interest in the electromechanical effects of doping. This is due to the possibility of driving the symmetry of BFO close to a morphotropic phase boundary, thereby enhancing its piezoelectric properties.^{15–17} There is, of course, a strong interest on the effect of doping on magnetic and magnetoelectric effects, with most studies focusing on the possibility of using doping in order to “unwind” the spiral spin structure of BFO in order to release the canted magnetic moment and enable linear magnetoelectric coupling.^{9,18}

Here we have doped BiFeO_3 with Ca, which has a smaller ionic size than Bi and may therefore be expected to act as a good proxy for hydrostatic pressure. Ca-doped BFO is beginning to attract attention as a doping element,^{8,19–22} both for applications such as catalytic membranes¹⁹ and for possible effects on magnetism.^{22,23} Doping with large divalent ions can lead to an unwinding of the spin spiral and release of canting magnetism, but Ca doping does not.²² However, it is not known how Ca substitution affects the magnetic-ordering temperature or how it relates to the properties of the parent compounds (BiFeO_3 and CaFeO_3) nor whether the charge-compensation mechanism (the valence of Ca^{+2} is different from that of Bi^{+3}) is the change in valence from Fe^{+3} to Fe^{+4} or the introduction of oxygen vacancies.

Here we have found that Ca doping increases the magnetic-ordering temperature ($T_{\text{Néel}}$), consistent with charge compensation by formation of O vacancies so that iron remains in the Fe^{+3} oxidation state. This implies that the change in magnetic-ordering temperature is exclusively due to structural effects and not to changes in the magnitude of the iron spin. The correlation between lattice contraction and increased $T_{\text{Néel}}$ therefore suggests that hydrostatic pressure should lead to an increase in $T_{\text{Néel}}$ in pure BiFeO_3 . The opposite effects of pressure (chemical or hydrostatic) on the ferroelectric- and magnetic-ordering temperatures may also be exploited to bring these two transitions closer together, thereby enhancing magnetoelectric coupling.

II. EXPERIMENT

The ceramic samples of Ca-BFO were synthesized following the recipe proposed by Ghosh *et al.*²⁴ 1:1 molar ratio $\text{Bi}(\text{NO}_3)_3$ and $\text{Fe}(\text{NO}_3)_3 \cdot 9\text{H}_2\text{O}$ was dissolved in water. To it, tartaric acid (molar ratio of metal to tartaric acid=1:1) was added to obtain a clear yellow-colored solution. The solution was evaporated at 100°C (boiling condition) under constant stirring in order to obtain a brownish solid precursor. The solid precursor was ground to make powder which was first dried in air in an oven at 100°C for another 24 h. Calcium doping was achieved by adding a stoichiometric amount of calcium nitrate in the starting solution. The precursor powder

was then calcined in air at 600 °C for 2 h. Pellets prepared from the calcined powder was sintered at 700 °C for 3 h in air. It was observed that, with increasing amount of calcium, the sintering temperature could be extended up to 850 °C without any noticeable phase separation. However, the sintering temperatures of all the samples were kept the same for the sake of consistency in the comparison of physical properties.

The lattice parameters of the ceramic were determined by x-ray powder diffraction at room temperature using a Bruker D8 diffractometer with Cu $K_{\alpha 1}$ radiation. Diffraction patterns were collected in θ - 2θ geometry from $2\theta=10^\circ$ – 150° . Lattice parameters were obtained from Rietveld refinement of the measured diffraction patterns using general structure analysis system.²⁵ The magnetic-ordering temperature was determined from specific heat and low-field ac susceptibility measurements. Heat-flow measurements were made through the Néel transition using a Perkin Elmer Diamond differential scanning calorimetry (DSC). Around 10 mg of powdered sample of each composition was enclosed in a Al sample can and run between room temperature and 773 K at a controlled heating rate with dry nitrogen purge. Temperature was calibrated against the melting temperatures of indium and zinc standards. Data from ten runs were combined to reduce noise, and poor-quality scans were eliminated from the data set. The Néel transition is accompanied by a significant peak in heat flow on heating, and the transition temperature was obtained from the point at which the first derivative of heat flow passed through zero. Magnetic-susceptibility measurements were carried out using an AGICO MKF1-FA kappa-bridge with an ac field of 200 A/m. Specimens were measured ten times up to ~ 440 °C (713 K) in air with a heating rate of 10 K/min. The Néel temperature was measured as the peak in the susceptibility signal on the heating run, as methods which determine the transition from the changes in gradient were imprecise due to noise.

III. RESULTS

The structure of BFO is rhombohedral at room temperature, and the influence of Ca doping is to reduce both the volume and the rhombohedral distortion of the unit cell. Figure 1 shows the pseudocubic lattice parameter of rhombohedral Ca-BFO plotted as a function of Ca concentration. As expected, the perovskite pseudocubic lattice parameter (defined as the cube root of the perovskite unit-cell volume) decreases with increasing Ca content. From a linear fit of the data, we obtain that the pseudocubic lattice parameter decreases at a rate of -0.003 Å per 1% mol of Ca doping. We have also analyzed the BFO pressure dependence of unit-cell volume reported by Gavriluk *et al.*⁵ and found that the pseudocubic unit-cell lattice parameter decreases at a rate of approximately -0.01 Å/GPa (we have only fitted pressures below ~ 10 GPa to avoid the high-pressure phase transitions^{5,7}). Based on this result, we make the association that, structurally at least, 1% Ca=0.3 GPa of chemical pressure.

We now turn to the effect of doping on the Néel temperature. Figure 2 shows a typical DSC measurement for a Ca-

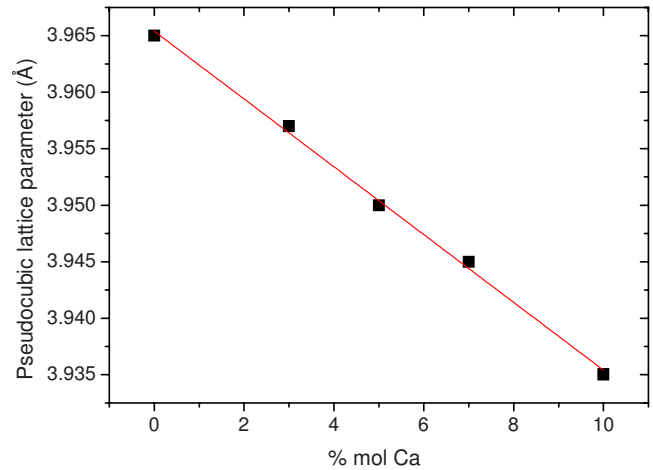


FIG. 1. (Color online) Evolution of the perovskite pseudocubic unit cell as a function of Ca concentration. The line is a least-squares fit to the experimental results, yielding a compression rate of -0.003 Å per 1% mol of Ca.

doped sample (7% Ca in this case); the Néel temperature shows up as a distinct peak. The inset of the figure shows the Ca-concentration dependence of $T_{\text{Néel}}$ as determined from the specific-heat measurements. It is found that T_N increases at about 0.66 K per 1% Ca. Combining this result with the chemical pressure equivalence (1% Ca=0.3 GPa), we estimate that $\partial T_N / \partial P \sim 2.2$ K/GPa of chemical pressure.

Figure 3 shows the magnetic susceptibility. Again, a distinct peak can be seen which we identify with $T_{\text{Néel}}$. Plotting this as a function of Ca concentration yields roughly the same result as the calorimetry measurements, although the 5% sample is off the trend in the magnetic measurements; this sample was observed to have an impurity phase of hematite (Fe_2O_3) so it is considered less reliable in terms of both stoichiometry and magnetic signal given the strong magnetism of hematite. From a linear fit of the data, we obtain that the Néel temperature increases at a rate of 0.6 K

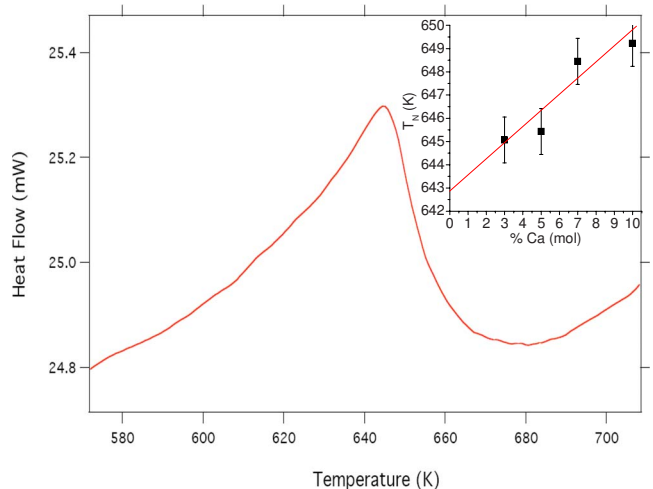


FIG. 2. (Color online) Differential scanning calorimetry of 7% Ca sample, showing a clear peak in specific heat at the Néel temperature. Inset: $T_{\text{Néel}}$ as determined from specific heat as a function of Ca concentration.

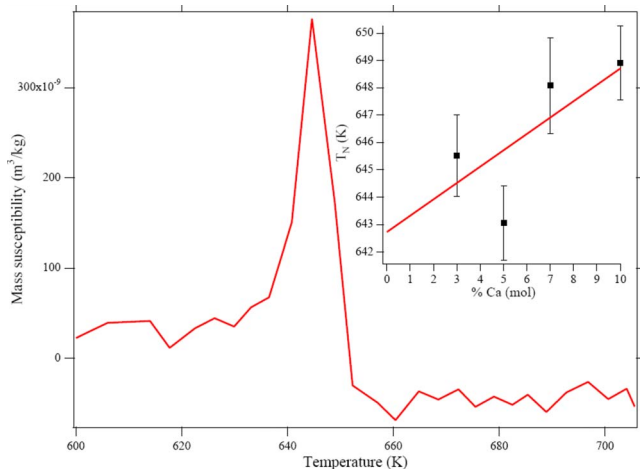


FIG. 3. (Color online) Magnetic ac susceptibility measurement for BFO-3% Ca, showing the distinct peak at the Néel temperature. Inset: T_N as a function of composition; the straight line is a least-squares fit.

per 1% Ca or $\partial T_N / \partial P \sim 2.0$ K/GPa of chemical pressure, which agrees well with the calorimetry result.

How do these results compare with the effect of real hydrostatic pressure? We know of no studies on the effect of hydrostatic pressure on the Néel temperature of BiFeO₃, but for perovskite orthoferrites the rate is²⁶ $\partial T_N / \partial P = 4\text{--}7$ K/GPa, which is comparable with—though somewhat bigger than—the effect of chemical pressure found in this work ($\partial T_N / \partial P \sim 2$ K/GPa). At this stage, it is not clear whether the difference is due to the fact that chemical pressure is not identical to hydrostatic pressure (the nonisovalent nature of the doping, Ca²⁺ for Bi³⁺, may induce changes in the electronic structure) or to the fact that the crystal structures of orthoferrites and BFO are different (orthoferrites are orthorhombic and BFO is rhombohedral). Direct measurements using real hydrostatic pressure are strongly encouraged and should answer this question.

IV. DISCUSSION

Ca²⁺ is, like Bi³⁺, a nonmagnetic ion, so it is not expected to contribute directly to the magnetic properties of this material. However, due to the different valence, doping BFO with Ca introduces a charge imbalance that must be equilibrated either by oxygen vacancies or by a change in the valence of iron from 3+ to 4+. Both charge-compensation mechanisms exist in nature and may, in principle, coexist in our samples. The brownmillerite structure (CaFeO_{2.5}) represents one extreme where all iron ions are Fe³⁺ and charge neutrality has been preserved purely by oxygen vacancies.^{27,28} On the other hand, vacancy-free CaFeO₃ can also be made with all irons in the 4+ state or a charge disproportionation of Fe³⁺ and Fe⁵⁺.^{29–31} These two extremes should in principle lead to very different outcomes for the magnetic-ordering temperature: Fe⁴⁺ has one less valence electron than Fe³⁺ and thus a smaller spin; the smaller spin of Fe⁴⁺ compound therefore have weaker magnetic interactions and lower-ordering temperature than the Fe³⁺ compound.

Let us first consider the scenario where charge neutrality is preserved by oxygen vacancies so that Fe³⁺ does not change its valence or its spin. A mixing rule suggests that the Néel temperature should simply evolve as the weighted average between the transition temperatures of BiFeO₃ and CaFeO_{2.5},

$$T_{\text{Néel}} = XT_{\text{Néel}}^{\text{CaFeO}_{2.5}} + (1 - X)T_{\text{Néel}}^{\text{BiFeO}_3}, \quad (1)$$

where X is the molar concentration of Ca in the mixture. According to this, the Néel temperature should increase 0.77 K per 1% mol of Ca doping. This is only marginally bigger than our experimentally measured values of 0.6–0.66 K per 1% mol Ca, suggesting that the charge compensation by oxygen vacancies is quite plausible. In contrast, the magnetic-ordering temperature of fully oxidized CaFeO₃ is only $T_{\text{Néel}} = 125$ K (Ref. 30), meaning that charge compensation by Fe⁴⁺ should lead to a substantial decrease in $T_{\text{Néel}}$, contrary to the observation. Therefore, oxygen vacancies are the dominant compensation mechanism.

Since the iron ions largely preserve their Fe³⁺ oxidation state, the changes in $T_{\text{Néel}}$ must be due to purely structural effects. These can be understood in the context of what is known about other perovskite iron oxides. BiFeO₃ has a rather exotic incommensurate magnetic structure,³² but its local spin structure is a conventional G -type antiferromagnet. This means that, on a local level, the magnetic properties of BFO are comparable to those of perovskite orthoferrites.^{33,34} In these, the strength of the antiferromagnetic superexchange interaction depends on the Fe-O-Fe angle ($\equiv \theta$); specifically, it is proportional to $\cos \theta$.^{35–37} The substitution of Bi by Ca has at least two structural effects. It contracts the lattice, as shown here, and it straightens the Fe-O-Fe bond angle.²¹ Both of these structural effects strengthen of the magnetic exchange and increase $T_{\text{Néel}}$, and both are expected to take place under real hydrostatic pressure.^{38,39}

The effect of doping may have useful consequences. As shown here, chemical pressure increases magnetic-ordering temperature. At the same time, hydrostatic pressure decreases the ferroelectric T_C : the paraelectric β phase above 1100 K is the same as the orthorhombic phase above 10 GPa at room temperature.^{4,7,40,41} For the right amount of pressure or doping, then, the two ferroic critical temperatures should coincide, leading to a maximization of magnetoelectric coupling.

The Néel temperature of BFO is 643 K, and it increases at a rate of 2.2 K/GPa, as shown here; the ferroelectric temperature, on the other hand, is 1100 K at ambient pressure and it decreases—roughly—at a rate of 80 K/GPa. The ferroelectric- and magnetic-ordering temperatures of pure BiFeO₃ should therefore coincide when $643 + 2.2P = 1100 - 80P$ (P expressed in GPa), i.e., when $P \sim 5.5$ GPa. We note parenthetically that a pressure of 5.5 GPa is in the middle of the range in which an intermediate monoclinic phase has been reported.⁷ This pressure represents a doping concentration of 18% Ca (mol). This, however, assumes that the Ca doping does not itself affect the chemical basis of the ferroelectricity, which is not true. Ferroelectricity in BFO depends on the lone-pair polarization of the Bi³⁺ ion, which is absent in Ca²⁺. Therefore, 18% mol is an overestimate of

the Ca concentration required to make $T_C = T_{\text{Néel}}$.

On the other hand, a side effect of Ca doping is that the sample conductivity becomes too high for the magnetoelectric properties to be directly measured. This is partly due to the mixed-valence nature of the compound, which introduces oxygen vacancies that act as donors. But there is also a structural effect on the conductivity. BiFeO₃ has a metal-insulator transition as a function of pressure and/or temperature,^{4,5} and this transition has been argued to be caused by gradual closing of the charge-transfer gap between O and Fe (Refs. 1, 4, and 41) due to bond-angle straightening.⁴¹ Accordingly, it is expected that the critical temperature of the metal-insulator transition should also decrease, and thus the conductivity increase, with Ca doping. Although the high-temperature transport studies are still underway, this prediction is consistent with the observation that pure CaFeO₃ displays a metal-insulator transition at ambient pressure and $T_{\text{MI}} \sim 115$ K (Ref. 30) compared with $T_{\text{MI}} \sim 1203$ K for pure BiFeO₃ (Ref. 4). An interesting exercise is to use the correlation between doping and pressure to regard CaFeO₃ as structurally equivalent to applying 33 GPa to BiFeO₃. Surprisingly for such a crude approximation, this is not far off the actual hydrostatic pressure required to induce the MI transition in BFO at low temperature,^{5,6} suggesting that the equivalence between chemical substitution and hydrostatic pressure is accurate.

V. CONCLUSIONS

In summary, Ca doping contracts the lattice of BFO and is in this respect similar to applying pressure. The Néel

temperature increases with Ca doping, and the correlation between chemical pressure and $T_{\text{Néel}}$ is consistent both with the decrease in Fe-Fe distance and the straightening of the Fe-O-Fe exchange angle.^{26,35–37} Based on this, it is argued here that chemical pressure can in principle be used as an effective means by which to tune the ferroelectric and magnetic transition temperatures so as to make them coincide, thereby enhancing magnetoelectric coupling. This magnetoelectric enhancement would be independent of that expected from the unwinding of the spin spiral.^{9,18} We expect the antiferromagnetic Néel temperature and the ferroelectric Curie temperature to coincide at pressures on the order of ~ 5.5 GPa or a doping concentration of $< 18\%$ mol Ca (upper limit).

However, due to the correlation between charge-transfer gap and Fe-O-Fe angle,⁴¹ we also expect that Ca doping will reduce both the conduction band gap and the metal-insulator transition temperature of BFO. Furthermore, the charge imbalance introduced by the nonisovalent doping is compensated by oxygen vacancies which act as charge donors that further increase conductivity. Any doping strategy aimed at increasing the magnetoelectric coupling via structural tuning of the exchange angle will therefore have to deal also with increased conductivity.

Note added in proof: Recently a new work was published⁴² reporting the interplay between ferroelectricity and conductivity in Ca-doped BFO thin films. Though magnetoelectric effects are not reported, the coupling between transport and polarization is maximum at a Ca concentration between 10–15%, i.e., just below the 18% upper limit estimated here for the crossover between T_C and $T_{\text{Néel}}$.

-
- ¹G. Catalan and J. F. Scott, *Adv. Mater.* **21**, 2463 (2009).
²J. Wang *et al.*, *Science* **299**, 1719 (2003).
³D. Lebeugle *et al.*, *Appl. Phys. Lett.* **91**, 022907 (2007).
⁴R. Palai *et al.*, *Phys. Rev. B* **77**, 014110 (2008).
⁵A. G. Gavriliuk *et al.*, *Phys. Rev. B* **77**, 155112 (2008).
⁶O. E. González-Vázquez and J. Íñiguez, *Phys. Rev. B* **79**, 064102 (2009).
⁷R. Haumont *et al.*, *Phys. Rev. B* **79**, 184110 (2009).
⁸M. Polomska *et al.*, *Phys. Status Solidi A* **23**, 567 (1974).
⁹Z. V. Gabbasova *et al.*, *Phys. Lett. A* **158**, 491 (1991).
¹⁰A. V. Zaleskii *et al.*, *Phys. Solid State* **45**, 141 (2003).
¹¹G. L. Yuan *et al.*, *J. Phys. D* **40**, 1196 (2007).
¹²J. R. Chen *et al.*, *J. Alloys Compd.* **459**, 66 (2008).
¹³X. Qi *et al.*, *Appl. Phys. Lett.* **86**, 062903 (2005).
¹⁴G. D. Hu *et al.*, *Appl. Phys. Lett.* **92**, 192905 (2008).
¹⁵J. R. Cheng and L. E. Cross, *J. Appl. Phys.* **94**, 5188 (2003).
¹⁶D. I. Woodward *et al.*, *J. Appl. Phys.* **94**, 3313 (2003).
¹⁷S. Fujino *et al.*, *Appl. Phys. Lett.* **92**, 202904 (2008).
¹⁸N. Wang *et al.*, *Phys. Rev. B* **72**, 104434 (2005).
¹⁹K. Brinkman *et al.*, *Jpn. J. Appl. Phys., Part 1* **46**, L93 (2007).
²⁰D. Kothari *et al.*, *Appl. Phys. Lett.* **91**, 202505 (2007).
²¹O. Troyanchuk *et al.*, *J. Exp. Theor. Phys.* **107**, 83 (2008).
²²V. A. Khomchenko *et al.*, *J. Appl. Phys.* **103**, 024105 (2008).
²³V. A. Khomchenko *et al.*, *Appl. Phys. Lett.* **90**, 242901 (2007).
²⁴S. Ghosh *et al.*, *J. Am. Ceram. Soc.* **88**, 1349 (2005).
²⁵A. C. Larson and R. B. Von Dreele, Los Alamos National Laboratory Report No. LAUR 86-748, 2000.
²⁶N. A. Halasa *et al.*, *Phys. Rev. B* **10**, 154 (1974).
²⁷E. F. Bertaut *et al.*, *Acta Crystallogr.* **12**, 149 (1959).
²⁸T. Takeda *et al.*, *J. Phys. Soc. Jpn.* **24**, 446 (1968).
²⁹F. Kanamaru *et al.*, *Mater. Res. Bull.* **5**, 257 (1970).
³⁰Y. Takeda *et al.*, *Mater. Res. Bull.* **13**, 61 (1978).
³¹M. Takano *et al.*, *Phys. Rev. Lett.* **67**, 3267 (1991).
³²I. Sosnowska *et al.*, *J. Phys. C* **15**, 4835 (1982).
³³C. Ederer and N. A. Spaldin, *Phys. Rev. B* **71**, 060401(R) (2005).
³⁴M. K. Singh *et al.*, *J. Phys.: Condens. Matter* **20**, 252203 (2008).
³⁵D. Treves *et al.*, *Phys. Lett.* **18**, 216 (1965).
³⁶A. Bombik *et al.*, *J. Magn. Magn. Mater.* **257**, 206 (2003).
³⁷J. S. Zhou and J. B. Goodenough, *Phys. Rev. B* **77**, 132104 (2008).
³⁸A. G. Gavrilyuk *et al.*, *J. Exp. Theor. Phys.* **90**, 330 (2000).
³⁹M. Medarde *et al.*, *Phys. Rev. B* **52**, 9248 (1995).
⁴⁰D. C. Arnold *et al.*, *Phys. Rev. Lett.* **102**, 027602 (2009).
⁴¹S. Redfern *et al.*, arXiv:0901.3748 (unpublished).
⁴²C.-H. Yang *et al.*, *Nature Mater.* **8**, 485 (2009).